Using thermal response factors with time dependent thermal properties

Stephan Düber[a,b,*], Raul Fuentes[a], Guillermo Narsilio Ferrero[b]

[a] *Institute of Geomechanics and Underground Technology, RWTH Aachen University, Mies-van-der-Rohe-Str. 1 Aachen, 52074, Germany*
[b] *Department of Infrastructure Engineering, The University of Melbourne, Parkville, Australia*

Abstract

This paper presents a simple and fast methodology to consider changing thermal properties in, for example, the design of shallow geothermal systems, by using thermal response factors. The simulation period is split into multiple sections according to the changes in thermal properties. By transforming the temperature response from one section to the next and subsequent superposition, any changes in the thermal conductivity properties of the media through which heat travels can be taken into account. The method is verified by numerical simulation and its efficiency is demonstrated in an application example. Results show that even though the computational effort increases exponentially with the variation of thermal parameters in time, the computational time is significantly shorter than comparable numerical simulations.

Keywords: Thermal response factor, g-function, thermal properties, variable conductivity, time dependent properties

---

1. Introduction

Thermal response factors, also known as g-functions [1], are one of the main methods for designing shallow geothermal systems such as borehole heat exchangers, energy piles or horizontal geothermal collectors. The g-functions describe the dimensionless, time-dependent thermal resistance of

*Corresponding author
Email address: dueber@gut.rwth-aachen.de (Stephan Düber)

the ground and allow the calculation of temperature changes due to heat conduction [2]:

$$\Delta T(t) = \frac{q}{2\pi\lambda} \cdot g(t). \tag{1}$$

Here λ is the thermal conductivity of the ground, q the thermal load, and g is the g-function of the heat exchanger, depending on its geometry and a dimensionless time. Starting from the infinite line source [2], more and more analytical approaches have been developed in recent years to calculate the g-functions. For borehole heat exchangers and energy piles, the heat source radius [3], finite length and surface effects [4, 5], groundwater flow [6], layered soil types [7] and more realistic interaction between multiple boreholes [8] can now be considered. Approaches for horizontal collectors can also take into account different geometries such as the slinky heat exchanger [9] and the finite length of the pipes [10].

All of the approaches described above assume though that the thermal properties of the ground are constant over time. This assumption is generally justified in many cases, especially for deeper systems. However, it may be too simplistic for e.g., horizontal geothermal collectors or even energy piles, since the thermal properties may vary because of ground moisture content fluctuations due to seasonal changes or climate change [11]. In these cases, time-demanding, more complex, numerical models are necessary to obtain an accurate response.

This paper fills this gap and presents a simple method to account for changing thermal properties using the thermal response factor method. The methodology is presented in detail in section 2, followed by a verification and application example in section 3, and finishing with conclusions in section 4. A Python implementation of the proposed method is available online.

2. Methodology

The proposed method works with any type of g-function, but for illustration purposes, we use here a single buried pipe, for which the g-function is calculated using the horizontal finite line source (HFLS) [10]:

$$g(t) = \int_{\frac{1}{\sqrt{4\alpha t}}}^{\infty} \frac{\left(e^{-r^2 s^2} - e^{-(r^2+4z^2)s^2}\right)}{Hs^2} \left[Hs\,\mathrm{erf}(Hs) - \frac{1}{\sqrt{\pi}}\left(1 - e^{-H^2 s^2}\right)\right] ds. \tag{2}$$

Here α denotes the thermal diffusivity of the ground, t the time, H the length of the line source, z its depth and r the horizontal distance where the temperature is evaluated. The temperature change $\Delta T(t)$ due to a time-varying thermal load $q(t)$ is calculated using the g-function method and the superposition principle [12] as:

$$\Delta T(t_k) = \frac{1}{2\pi\lambda} \sum_{i=1}^{k} \Delta q(t_i) \cdot g(t_{k-i+1}) \tag{3}$$

where $\Delta q(t_i) = q(t_i) - q(t_{i-1})$ is the load increment, λ is the thermal conductivity of the ground and g the g-function according to Equation 2.

Neither Equation 3 nor the formulation of the g-function account for time dependent thermal properties of the ground. It means that, applying Equation 3 for a constant load $q(t)$ for $t_{\text{start}} \leq t \leq t_{\text{c}}$ results in a $\Delta T(t)$ as shown in the top part of Figure 1.

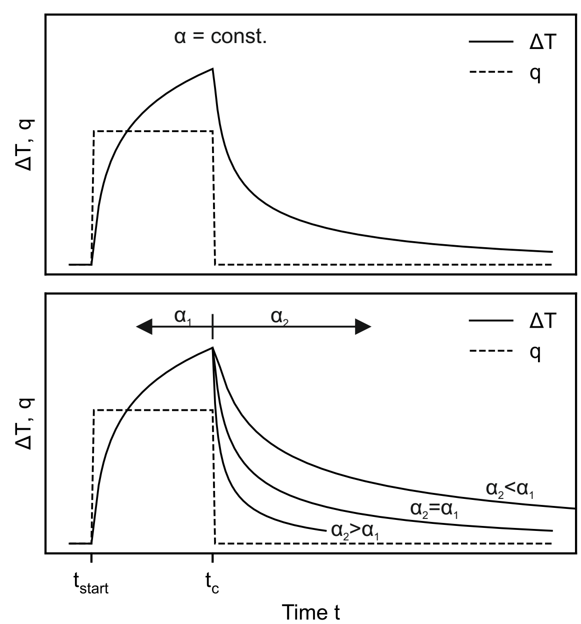

Figure 1: Temperature change ΔT according to a constant load q between t_{start} and t_{c} for a typically assumed constant thermal parameter α of the heat transfer medium (top) and for the case when α changes for $t > t_{\text{c}}$ (bottom).

However, in reality, the thermal properties of the ground can change. Hence, if the thermal diffusivity α of the ground changes instantaneously at

$t = t_c$, this change will only affect the temperature decay for $t > t_c$, as shown conceptually in the bottom part of Figure 1.

As the temperatures for $t > t_c$ have been calculated using Equation 3 for α_1, we suggest that there is no need to recalculate them for α_2. In fact, we propose that the change of α only causes a compression or stretching of the already calculated temperature change along the time axis. Hence, we can write for $t > t_c$:

$$\Delta T(\alpha_2, t) = \Delta T(\alpha_1, t\frac{\alpha_1}{\alpha_2} - t_c(\frac{\alpha_1}{\alpha_2} - 1)). \tag{4}$$

The factor $\frac{\alpha_1}{\alpha_2}$ accounts for a time stretching/compression of the temperature curve while $t_c(\frac{\alpha_1}{\alpha_2} - 1)$ corrects for the thereby introduced offset.

Figure 2 shows conceptually what happens if the thermal property reduces from α_1 to α_2 at time $t = t_c$ (see solid line). The temperature will grow faster from $t = t_c$ until the time when $q = 0$, from which it will start a normal decay. The resulting curve is the superposition of the ΔT calculated using Equation 3 for α_1, from $t = t_{\text{start}}$ to $t = t_c$, plus the same temperature response transformed for $t > t_c$, plus one calculated for α_2 from $t = t_c$ onward.

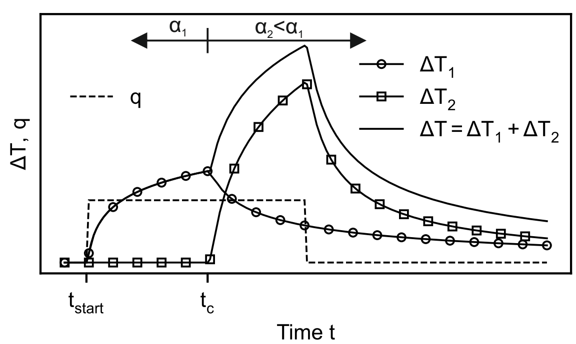

Figure 2: Temperature change for a constant load with changing α at t_c as the sum of ΔT_1 and ΔT_2.

The method described can be used for any type of thermal load profile and for any variation in thermal conductivity or heat capacity. For an efficient implementation, we use the Fast Fourier Transform (FFT) as presented by [13], which replaces the summation over time in Equation 3 with a single multiplication in the Fourier domain:

$$\Delta T = \mathscr{F}^{-1}\left(\mathscr{F}\left(\frac{\Delta q}{2\pi\lambda}\right)\cdot\mathscr{F}(g)\right) \tag{5}$$

where $\mathscr{F}$ is the direct and $\mathscr{F}^{-1}$ the inverse FFT. To ensure that Equation 4 can be applied for any change in α, the simulation period must be extended. An increase in α results in a compression of the temperature response along the time axis, as can be seen in the bottom part of Figure 1. To ensure that the transformed temperature response covers the entire simulation period, the maximum time t_{max} must be increased to t'_{max} as:

$$t'_{\mathrm{max}} = \max(\{f(\alpha_j) : j = 1, \ldots, n\}) \tag{6}$$

with:

$$f(\alpha_j) = \frac{1}{\alpha_j}\left(\sum_{i=j}^{n-1}\alpha_i t_{\mathrm{c},i+1} - \sum_{i=j+1}^{n}\alpha_i t_{\mathrm{c},i} + \alpha_n t_{\mathrm{max}}\right) \tag{7}$$

where n stands for the number of changes in α and $t_{\mathrm{c},i}$ for the times at which α changes. Finally, the implementation follows the flowchart presented in Figure 3.

3. Verification and application

To verify the described approach, we compare it to a simulation using a 2D numerical finite volume model. The numerical model is spatially discretised with 600×600 cells each 10×10 mm in size. The temperatures on the cell walls are calculated using the central difference scheme while the explicit Euler scheme is used for the numerical integration. All parameters and boundary conditions are listed in Table 1. A large value was chosen for the length of the line source to minimise the influence of the finite length, which is not considered in the 2D numerical model. The radius in Table 1 denotes the horizontal distance from the line source where the temperature is evaluated. Using two thermal property changes over the calculation period, the results in Figure 4 show perfect agreement between the numerical simulation and our approach. The numerical simulation took 181 s on a standard personal computer, while the computational time for the analytical approach was just 1.5 s.

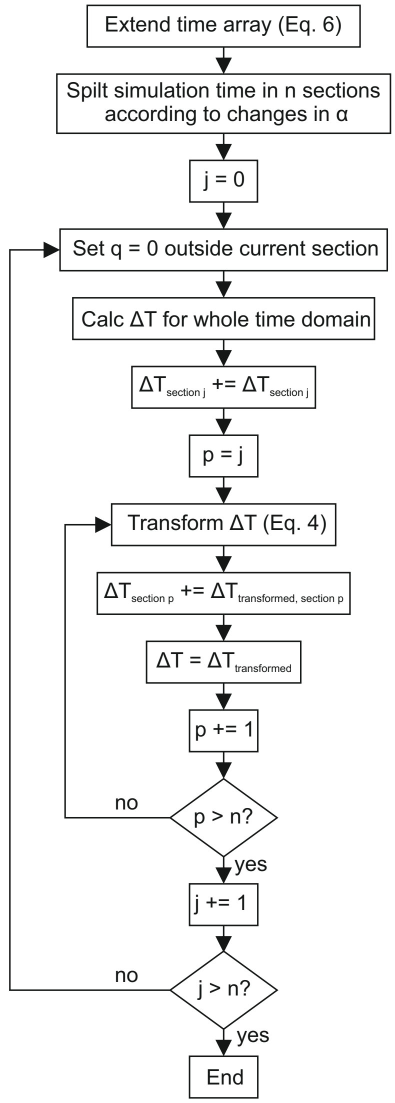

Figure 3: Flowchart for the algorithm to account for arbitrary variations of α.

To show how the method performs for a realistic scenario, we consider a single pipe of a horizontal geothermal collector buried 1.2 m below the surface exposed to the hourly load profile shown in Figure 5. The load profile is derived from measurements of an operating geothermal system in Germany, all other parameters are given in Table 2.

For the ground it is assumed that the thermal properties change sea-

Table 1: Parameters used for verification simulation.

Parameter	**Symbol**	**Value**	**Units**
HFLS length	H	500	m
HFLS depth	z	0.85	m
Radius	r	0.2	m
Thermal load	q	30	$\mathrm{W\,m^{-1}}$
Thermal conductivity	λ	1.0 for $t < t_{c,1}$ 2.0 for $t_{c,1} \leq t < t_{c,2}$ 1.5 for $t \geq t_{c,2}$	$\mathrm{W\,m^{-1}\,K^{-1}}$
Volumetric heat capacity	ρc	1 000 000	$\mathrm{J\,m^{-3}\,K^{-1}}$
Simulation time	$t_{\max}$	35	h
Time step	Δt	12.5	s
Time of change 1	$t_{c,1}$	41 675	s
Time of change 2	$t_{c,2}$	83 337.5	s

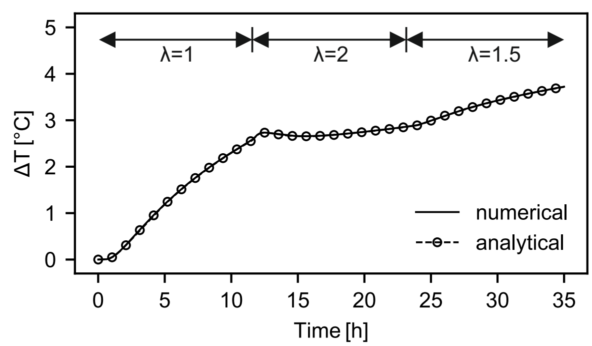

Figure 4: Comparison of the proposed method with and numerical finite volume simulation.

sonally due to a change in the water content of the ground. The ground water content over central-western Europe can be approximated with a sinusoidal curve [14]. Here we assume for the thermal conductivity λ a value of $1.0\,\mathrm{W\,m^{-1}\,K^{-1}}$ for the dry and $2.2\,\mathrm{W\,m^{-1}\,K^{-1}}$ for the fully saturated case. The volumetric heat capacity ρc is considered to be $1.5\,\mathrm{MJ\,m^{-3}\,K^{-1}}$ for the dry and $2.2\,\mathrm{MJ\,m^{-3}\,K^{-1}}$ for the fully saturated case, resulting in the profile shown in Figure 6. To understand the importance of ground property variations, we approximate the profile of the thermal properties with daily,

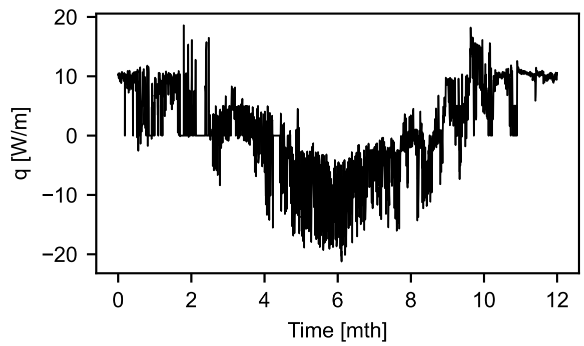

Figure 5: Hourly load profile used for the application example.

Table 2: Parameters used for the application example.

Parameter	**Symbol**	**Value**	**Units**
HFLS length	H	20	m
HFLS depth	z	1.2	m
Radius	r	0.02	m
Thermal conductivity	λ	see Figure 6	
Volumetric heat capacity	ρc	see Figure 6	
Simulation time	$t_{\max}$	8760	h
Time step	Δt	1200	s

monthly and three-monthly averages, resulting in 4, 12 and 365 values for α in the simulation. As we are only interested in the effect of the changes in the thermal properties, we neglect the course of the undisturbed ground temperature and restrict the analysis to the temperature change at the outside of the pipe introduced by the heat exchanger.

The top part of Figure 7 shows the results for the simulation with averaged thermal properties ($\lambda = 1.6\,\mathrm{W\,m^{-1}\,K^{-1}}$, $\rho c = 1.85\,\mathrm{MJ\,m^{-3}\,K^{-1}}$) for the whole simulation period as reference. The lower parts show the temperature difference introduced by considering the different time resolution for changes in thermal properties. For the scenarios with 4 and 12 different values of α, the changes are clearly visible compared to the smooth curve for 365 values of α. The temperature difference introduced by the change in thermal properties is more than 2 °C, which is almost half of the temperature change

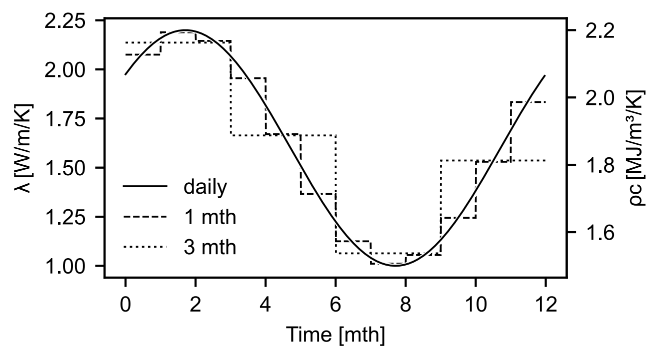

Figure 6: Sinusoidal approximation of annual profile of the thermal properties. Daily, monthly and 3 monthly averaged values used as input for the simulation.

caused by the heat exchanger when considering averaged properties (Figure 7, top).

Finally, as Table 3 shows, the computational times of the model increase exponentially with the number of changes in α. This is because for each change, the response has to be transformed (Equation 4) for all subsequent values of α. However, even with daily updated values the total computation time is still only 44.8 s, clearly superior to numerical simulations.

Table 3: Computational times depending on the number of values for α.

n_α	comp. time [s]
1	0.017
4	0.065
12	0.31
365	44.8

4. Conclusions

The use of thermal response factors is widespread in the simulation of shallow geothermal systems. While the thermal properties of the ground are rightly assumed to be constant for the simulation of borehole heat exchangers, typically 100 m or deeper, they can vary closer to the surface for a number of reasons over the life-time operation. This change, caused, for example, by varying groundwater levels or moisture content, can be relevant for systems such as horizontal geothermal collectors or shorter energy piles.

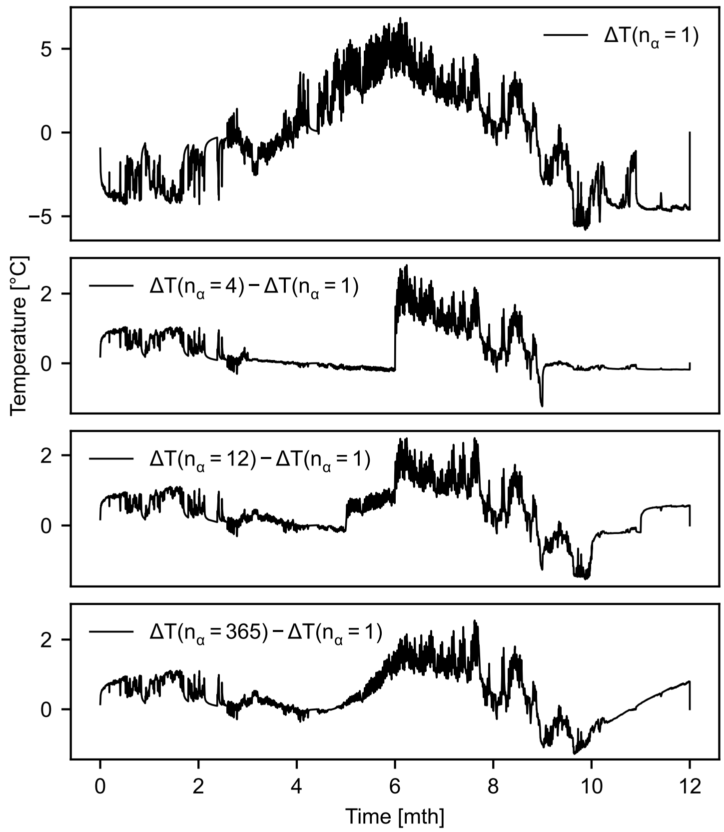

Figure 7: Results of the application example with n_α values for α for the simulation period.

The proposed approach is a simple, yet efficient, method to account for changing thermal properties using the response factor method. By dividing the simulation domain into several sections according to the changes in thermal properties and applying the superposition principle, arbitrary variations in thermal properties can be considered. The computational effort increases exponentially with the number of changes, but it is still considered superior to numerical simulations in many cases.

References

[1] P. Eskilson, Thermal analysis of heat extraction boreholes [ph. d. thesis], Lund, Sweden: University of Lund (1987).

[2] L. Ingersoll, O. Zobel, A. Ingersoll, Heat Conduction: With Engineering, Geological, and Other Applications, McGraw-Hill, New York, 1954.

[3] Y. Man, H. Yang, N. Diao, J. Liu, Z. Fang, A new model and analytical solutions for borehole and pile ground heat exchangers, International Journal of Heat and Mass Transfer 53 (13-14) (2010) 2593–2601.

[4] H. Y. Zeng, N. R. Diao, Z. H. Fang, A finite line-source model for boreholes in geothermal heat exchangers, Heat Transfer—Asian Research: Co-sponsored by the Society of Chemical Engineers of Japan and the Heat Transfer Division of ASME 31 (72) (2002) 558–567.

[5] J. A. Rivera, P. Blum, P. Bayer, A finite line source model with cauchy-type top boundary conditions for simulating near surface effects on borehole heat exchangers, Energy 98 (2016) 50 – 63, cited by: 44; All Open Access, Bronze Open Access. doi:10.1016/j.energy.2015.12.129.

[6] N. Molina-Giraldo, P. Blum, K. Zhu, P. Bayer, Z. Fang, A moving finite line source model to simulate borehole heat exchangers with groundwater advection, International Journal of Thermal Sciences 50 (12) (2011) 2506–2513.

[7] S. L. Abdelaziz, T. Y. Ozudogru, C. G. Olgun, J. R. Martin, Multilayer finite line source model for vertical heat exchangers, Geothermics 51 (2014) 406–416. doi:https://doi.org/10.1016/j.geothermics.2014.03.004.

[8] M. Cimmino, M. Bernier, A semi-analytical method to generate g-functions for geothermal bore fields, International Journal of Heat and Mass Transfer 70 (2014) 641–650.

[9] H. Li, K. Nagano, Y. X. Lai, A new model and solutions for a spiral heat exchanger and its experimental validation, International Journal of Heat and Mass Transfer 55 (15-16) (2012) 4404–4414. doi:10.1016/j.ijheatmasstransfer.2012.03.084.

[10] L. Lamarche, Horizontal ground heat exchangers modelling, Applied Thermal Engineering 155 (2019) 534–545. doi:10.1016/j.applthermaleng.2019.04.006.

[11] W. Leong, V. Tarnawski, A. Aittomäki, Effect of soil type and moisture content on ground heat pump performance: Effet du type et de l'humidité du sol sur la performance des pompes à chaleur à capteurs enterrés, International Journal of Refrigeration 21 (8) (1998) 595–606.

[12] H. S. Carslaw, J. C. Jaeger, Conduction of heat in solids, Oxford University (1959).

[13] D. Marcotte, P. Pasquier, Fast fluid and ground temperature computation for geothermal ground-loop heat exchanger systems, Geothermics 37 (6) (2008) 651–665.

[14] E. Van der Linden, R. Haarsma, G. Schrier, Impact of climate model resolution on soil moisture projections in central-western europe, Hydrology and Earth System Sciences 23 (2019) 191–206. doi:10.5194/hess-23-191-2019.